DOI: 10.18462/iir.icr.2023.0958

Design And Optimization of Niobium-Titanium Based Superconductive Magnet for The Magneto Resistive Heat Switch

B. Kiran Naik [(a)]*, Shivendra Kr Rathore[(a)], Yash Desale[(a)], K.S. Patel[(b)], Suryanarayan Dash[(c)], and V. K. Singh[(d)]

[(a)]Sustainable Thermal Energy Systems Laboratory (STESL), Department of Mechanical Engineering, National Institute of Technology Rourkela, Rourkela, Odisha – 769008, India

[(b)]Department of Mechanical Engineering, National Institute of Technology Rourkela, Rourkela, Odisha – 769008, India

[(c)]Department of Physics and Astronomy, National Institute of Technology Rourkela, Rourkela, Rourkela, Odisha – 769008, India

[(d)]Thermal Engineering Division, Space Applications Centre, ISRO, Ahmedabad – 380015, India

*Corresponding author: naikkb@nitrkl.ac.in ; k.bukke@gmail.com ; Ph. No.: +91 9435686059

ABSTRACT

A superconducting magnet is an ordinary electromagnet with no current resistance. To attain the superconducting state, it is necessary to hold the material below its critical temperature. There are three types of superconducting magnets viz., low-temperature, medium-temperature, and high-temperature superconductors with an operating temperature range of 4.2K, 20K, and 100K, respectively. This work addresses the design and optimization of 6T LTS magnets for use in an adiabatic demagnetization refrigerator. LTS utilizes a Niobium-Titanium alloy wire that can generate a magnetic field between 3 T and 10 T. NbTi wires are wrapped around a hollow metal cylinder called a former. The surrounding coils are kept at a cryogenic temperature of 4.2K. A hollow cylindrical base with NbTi wires wrapped around it serves as a solenoid. In this study, the characteristics that affect the design and optimization of the length of the former, the diameter of the coil, the number of turns necessary to generate a 6 T magnetic field, and the required current are examined by developing an analytical model. 304L-grade stainless steel is considered as solenoid/former material in the present investigation. The optimal length and diameter of the former are determined by developing analytical model. Various situations are addressed by adjusting the wire's length, number of turns, and current, which results in a change in magnetic field density. Further, by developing a numerical model, type of superconducting alloy wire preferred below 9 K is also studied in detail.

Keywords: Numerical and analytical models, low-temperature superconducting magnet, NbTi wire, central and critical fields, number of turns.

1. INTRODUCTION

There are certain materials that exhibit a unique property which cooled down to very low temperatures shows zero resistivity, such unique property is termed as superconductivity. There is a certain temperature limit below which these materials start behaving as superconducting materials and that temperature is known as critical temperature TC. Every material has its own critical temperature depending on material properties and when they achieve required temperature that material starts to behave as a superconductor having zero resistivity. Apart from this, there are two other parameters which are considered to determine whether the material is in superconducting state or normal conducting state i.e., critical current density JC and critical magnetic field BC [1].

For space applications, electromagnets today are being replaced by superconducting Magnets due to their less weight & less space consumption; it has cryogenic support systems & can be operated reliably without human interference with possibility of very low heat leak & also capable of operating in a zero–gravity environment in space [2]. Apart from the above reasons, it should also be noticed that the low temperatures can be used for superconductivity has its own benefits. Based on critical temperature, superconducting magnets can be classified as low temperature superconducting (LTS) and High Temperature superconducting (HTS). LTS have superconducting wires such as NbTi (Tc–9.5K), Nb3Sn (Tc–18.3K) and Nb3Al (Tc–18.5K) [3,4]. High Temperature superconducting (HTS) magnets are fabricated with Rare-Earth Barium Copper Oxide (REBCO) and Bismuth Strontium Calcium Copper Oxide (BSCCO). Both these superconducting tapes have a critical temperature in the range of 100K. The difference between these two types is that LTS requires Liquid Helium or expensive cryo-coolers to maintain the critical temperature of the superconducting wires, whereas HTS on the other hand have a high critical temperature. Hence, no liquid helium or cryo-coolers is required which makes HTS an inexpensive superconducting magnet [5, 6].

In a normal conductor, the electrons are free to move around, and they can collide with the lattice of ions in the material, causing resistance to the flow of electrical current. In a superconductor, the electrons pair up and form Cooper pairs, which are held together by the lattice vibrations (phonons). These pairs move freely through the material without any resistance. Figure 1 depicts the superconducting magnet.

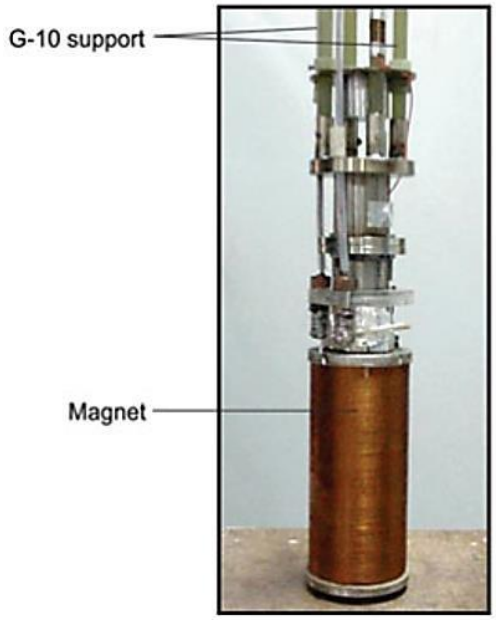

Figure 1: 3D view of superconducting magnet [7]

1.1. Literature gap

From the literature, it is found that mathematical and numerical analyses were performed at cryogenic temperatures on the LTS magnets comprising of NbTi superconducting wires [8]. In addition, an investigation and optimization of a lightweight former made of stainless steel of grade 304L was carried out utilising numerical methods [9]. A review of the relevant scientific literature indicates that none of the researchers have proved how the magnetic field changes with change in coil size or current, or in response to variations in the number of turns on the coil. There has been some experimental research carried out on superconducting magnets. However, numerical simulations, has not been carried out in this till date. Furthermore, an optimal coil dimensions, number of turns, and the current predictions that can be chosen by performing parametric and performance studies is yet to be explored. Therefore, in this study, by developing the analytical and numerical models, the performance of the superconducting magnet is investigated in detail for various coil dimensions, cryogenic temperature, and current. Moreover, effect of

various superconducting alloy wires that can be considered for below 9 K cryogenic temperature is also investigated in detail.

2. MATHEMATICAL MODELING

To design the superconductive magnet, two theoretical models are developed. They are analytical model and COMSOL simulation based numerical model. The uniqueness of the proposed models compared to the pre-deigned models reported in the literature [10-16] are visualising and analysing the influence of cryogenic temperature, magnetic field and current along the transverse and radial directions of the superconductive magnet, studying effect of former length on design of superconductive magnet, reduces the cost etc. Niobium Titanium and 304L stainless steel materials are chosen as superconducting wire and metal former, respectively. The dimensions, operating conditions and their range considered for the present study are provided in Table 1. Assumptions of the developed models are as follows,

- The model selected is stationary
- Coil winding over SS 304 L is considered a perfect cylindrical geometry.
- A static magnetic field is produced when direct current is passed through a solenoid

Table 1. Operating range and inlet condition

Parameter	Range	Inlet condition
Coil	LTS	LTS
Material used	NbTi	NbTi
Type of winding	Circular	Circular
Inner diameter (mm)	50 - 100	80
Outer diameter (mm)	110 - 150	120
Coil height (mm)	100 - 200	100
Total no. of turns	15924	-
Operating current (A)	6 - 200	30
Operating temperature (K)	3.5 – 9.5	4.2
Peak field (T)	3.88	-
Central field (T)	6.04	-
Current density (A/mm^2)	199.74	199.74

The radial field of an infinitely long solenoid is given by Eq. (1) as follows,

$$B_0 = J\lambda a_1 F(\alpha, \beta) \qquad \text{Eq. (1)}$$

where B_0 is the mid-plane axial field, J is the conductor's current density, and λ is the space factor, which typically varies between 0.70 and 0.90 based on the voids in the winding and the usage of non-superconducting materials such as multilayer insulation, etc.

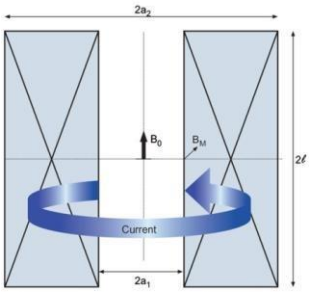

Figure 2: Schematic view of solenoid with the dimensions $2a_1$, $2a_2$, and a winding length of 2l

Here, α = a_2/a_1 is the ratio of the external winding diameter to the internal winding diameter, β = $2l/2a_1$, is the ratio of the winding height to the internal winding diameter, the field factor F(α, β), is a geometrical quantity also known as the field factor or shape factor, or Fabry parameter, and is described by Eq. (2) as follows:

$$F(\alpha,\beta) = \mu_0\beta \ln\left[\frac{\alpha + (\alpha^2+\beta^2)^{\frac{1}{2}}}{1 + (1+\beta^2)^{\frac{1}{2}}}\right] \quad \text{Eq. (2)}$$

2.1 Governance parameters

2.1.1 Biot Savart Law:

The Biot-Savart Law states that the magnetic field at a particular position P, caused by a current element, is given by,

$$\vec{dB} = \frac{1}{4\pi\varepsilon_o c^2} i \frac{\vec{dl} \times \vec{r}}{r^3} \quad \text{Eq. (3)}$$

Here 'c' is the speed of the light, 'i' is the current, $\vec{dl}$ is length – vector of the current element to the point P. The quantity $\frac{1}{s_0 c^2}$ is written as μ_o and it is called as the vacuum permeability. This permeability of vacuum μ_o is having a value of $4\pi \times 10^{-7}$. Eq. (3) is simplified and is given by Eq. (4),

$$\vec{dB} = \frac{\mu_o}{4\pi} i \frac{\vec{dl} \times \vec{r}}{r^3} \quad \text{Eq. (4)}$$

Equation 4 is the mathematical form of Biot–Savart Law & the magnitude of the field is given by Eq.(5)

$$dB = \frac{\mu_o}{4\pi} \frac{i dl \sin\theta}{r^2} \quad \text{Eq. (5)}$$

where θ is the angle between $\vec{dl}$ & $\vec{r}$

2.1.2 Ampere's Circuital law:

Calculating the magnetic field that results from a specific current distribution can also be done with the help of this other approach. When any closed plane curve is taken into consideration, a feeling can be assigned to the curve by maintaining an arrow along the curve. The equation that expresses Ampere's law is given by Eq. (6),

$$\oint \vec{B}.\vec{dl} = \mu_o i \quad \text{Eq. (6)}$$

where $\vec{B}$ is the resultant magnetic field at the position of $\vec{dl}$. It can be further expressed as Eq. (7):

$$B = \frac{\mu_0 NI}{l} \quad \text{Eq. (7)}$$

3. NUMERICAL MODELING

3.1 Governing Equations

The geometry is generated using COMSOL's built-in function, and then the material for the Former is selected using user-defined input. The built-in equation for Ampere's Law is used for this investigation given by Eq. (8),

$$\nabla \times H = J \quad \text{Eq. (8)}$$

This equation can be further expressed as Eq. (9),

$$\left(\frac{\partial H_z}{\partial y} - \frac{\partial H_y}{\partial z}\right)\bar{a}_x + \left(\frac{\partial H_x}{\partial z} - \frac{\partial H_z}{\partial x}\right)\bar{a}_y + \left(\frac{\partial H_y}{\partial x} - \frac{\partial H_x}{\partial y}\right)\bar{a}_z = J \quad \text{Eq. (9)}$$

where 'H' indicates magnetic field intensity and 'J' denotes applied current density. Another equation that is used for simulation is given by Eq. (10),

$$B = \nabla \times \mathrm{A} \quad \text{Eq. (10)}$$

This equation can be given by Eq. (11),

$$B = \left(\frac{\partial A_z}{\partial y} - \frac{\partial A_y}{\partial z}\right)\bar{a}_x + \left(\frac{\partial A_x}{\partial z} - \frac{\partial A_z}{\partial x}\right)\bar{a}_y + \left(\frac{\partial A_y}{\partial x} - \frac{\partial A_x}{\partial y}\right)\bar{a}_z \quad \text{Eq. (11)}$$

where B represents the magnetic flux intensity and A represents the vector potential.

Also, there is one another equation which is also being used in this study which is given as, Eq. (12)

$$\vec{J} = \sigma \vec{E} \quad \text{Eq. (12)}$$

Here $\vec{J}$ is the current density σ is the conductivity & $\vec{E}$ is the electric field.

3.2 Boundary Conditions

Magnetic insulation is applied to the entire cylinder geometry that surrounds the hybrid coil. This magnetic insulation is expressed by an equation given as, Magnetic insulation is applied to the entire cylinder geometry that surrounds the hybrid coil. This magnetic insulation is expressed by an equation given as, Eq. (13)

$$\boldsymbol{n} \times \boldsymbol{A} = \mathbf{0} \quad \text{Eq. (13)}$$

Operating temperature for this numerical study is set at 4.2 K. and maximum current applied during the study is 30 A.

3.3 Meshing

For the performance analysis of the superconducting magnet using the developed numerical model based on COMSOL Multiphysics, the optimal mesh elements are observed to be 97,102.

4. MODEL VALIDATION

To utilize the developed analytical and numerical models with confidence validation is essential. Therefore, in the present study, the developed models are validated with the experimental data available in the literature as shown in Figs. 3 and 4 [7]. From this figure, it is found that the developed models are in line with the experimental data with a maximum possible deviation of ±13% and ±8.3% for the analytical and numerical models, respectively. Further, Figs. 3 and 4 shows the variation of central field with current. From this figure,

it is analyzed that for a given operating condition available in the literature (Table 1), as the current increases from 0 A to 200 A, the magnetic flux density observed to increase.

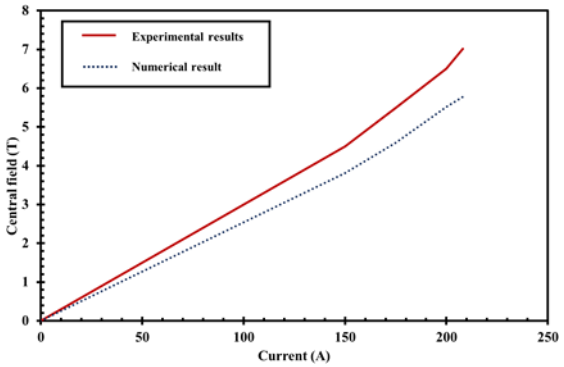

Figure 3: Comparison between present numerical model and experimental data

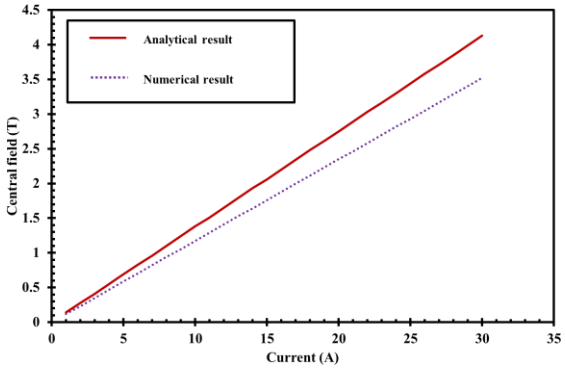

Figure 4: Comparison between analytical and numerical result for 200 mm coil height

5. PARAMETRIC INVESTIGATION AND PERFORMANCE ANALYSIS

For a given operating condition and range as well as specifications presented in Table 1, a detailed parametric investigation and performance analysis on the superconducting magnet is carried out using the developed analytical model by varying one inlet parameter arbitrarily and keeping rest of them as constant. The performance parameters considered for this study are central field, number of turns and critical field whereas inlet parameters chosen are coil height, current, space factor and cryogenic temperature. Fig. 5 – 8 shows the effect of coil height, magnetic field and current on number of turns, coil height and current on central field, coil height, cryogenic temperature and current on critical field and space factor and cryogenic temperature on critical field. Following results are observed from the parametric study and performance evaluation:

(a) For a given magnetic field and current, by increasing coil height from 10 cm to 20 cm, the number of turns required found to increase linearly (Fig. 5). This indicates that requirement of coil winding tends to increase. Further, for the provided current and coil height, with increase in magnetic field from 1.5 T to 6 T, required number of turns observed to increase. This happens because as the number of windings increases, flow of electrons causing current increases, which interim raises the magnetic field strength. In addition, it is analysed that for a particular applied magnetic field and coil height, with increase in current from 6 A to 30 A, the required no. of turns increases. This suggests that there is a requirement of more coil winding to generate high magnetic field.

(b) For a particular current and magnetic field, with increase in cryogenic temperature from 1.5 K to 7.5 K and coil height from 10 cm to 20 cm, the critical field observed to decrease logarithmically (Fig. 6). It occurs due to the reduction in superconducting behaviour of the NbTi alloy when the cryogenic temperature nears to its critical temperature. Moreover, it is assessed that as the current increases from 6 A to 30 A for the given cryogenic temperature, magnetic field, and coil height, the critical field found to increase. It happens because raise in magnetic field strength is directly proportional to the current.

(c) As the coil height increases from 10 cm to 20 cm for the given current, the central field observed to decrease whereas with increase in current from 6 A to 30 A, the central field is found to increase (Fig. 7). From this analysis, it is understood that as the current increases and coil height decreases, electrons accumulation increases by which potential for magnetic field increases.

(d) With increase in space factor from 0.7 to 0.9 and cryogenic temperature from 3.5 K to 9.5 K, the critical field tends to increase (Fig. 8). This is because as the space factor increases, the former cross-section increases and coil winding cross-section decreases. As a result, critical field observed to decrease.

(e) Further, from Figs. 5–8, it is found that 6T is the maximum magnetic field that can be generated for the given operating condition. Accordingly, the optimal inlet conditions for the maximum magnetic field generated is presented in Table 2.

Table 2. Optimal inlet condition

a_1 (mm)	a_2 (mm)	λ	No. of turns	Coil height cm	Current A
50	120	0.9	15924	100	30

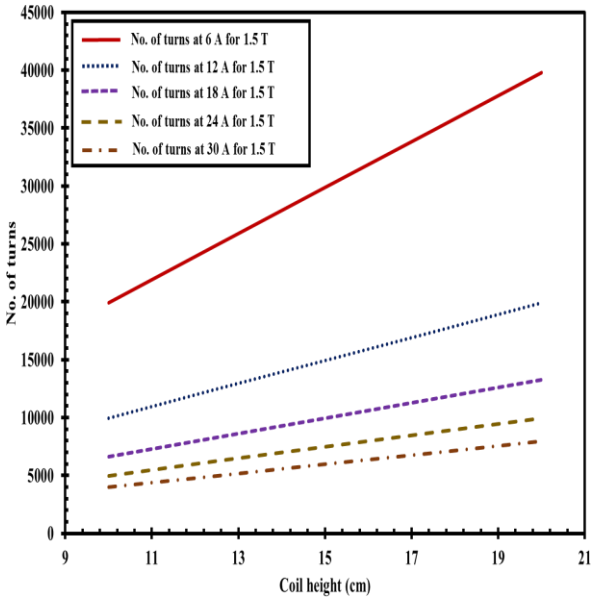

(a) No.of turns at 1.5 T

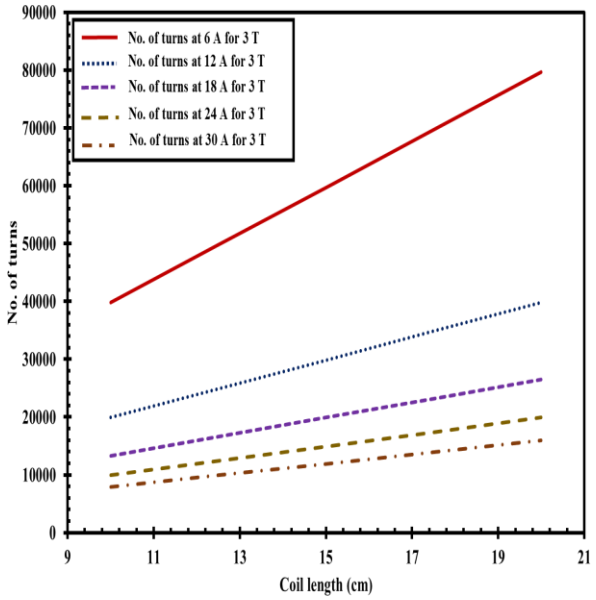

(b) No.of turns 3 T

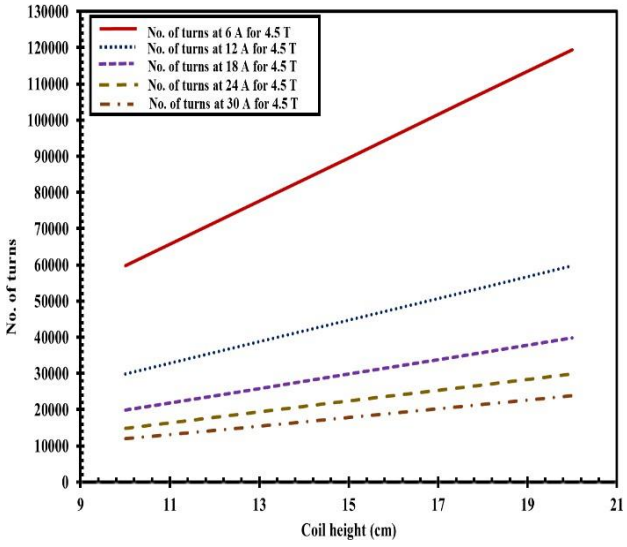

(c) No.of turns at 4.5 T

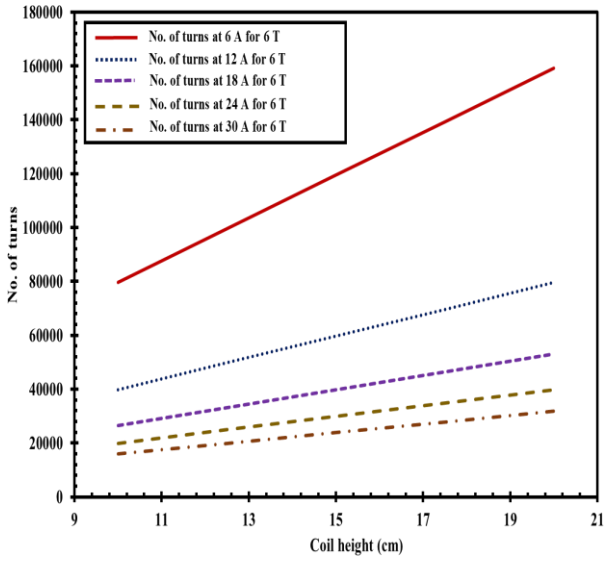

(d) No.of turns at 6 T

Figure 5: Variation of no. of turns with coil height

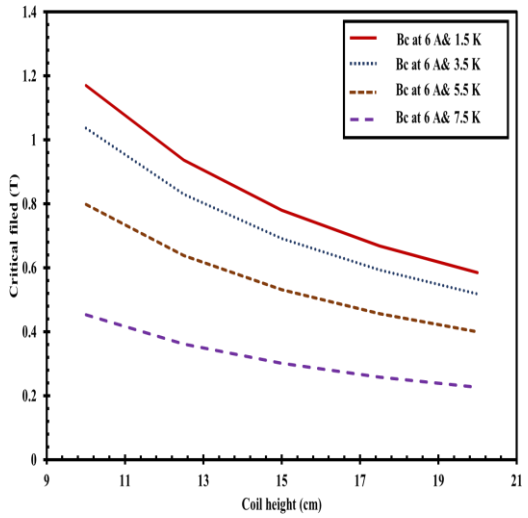

(a) Critical field at 6 A

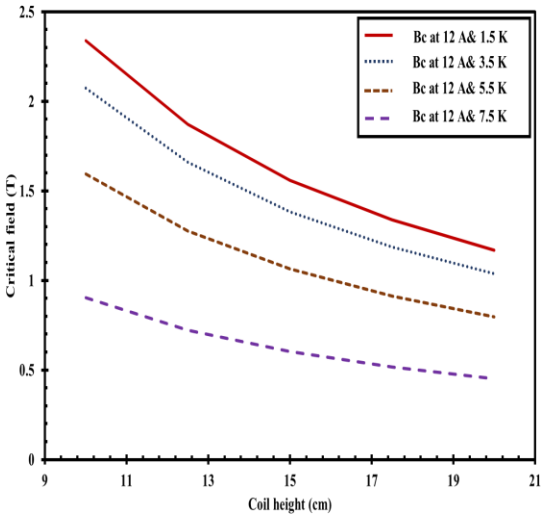

(b) Critical field at 12 A

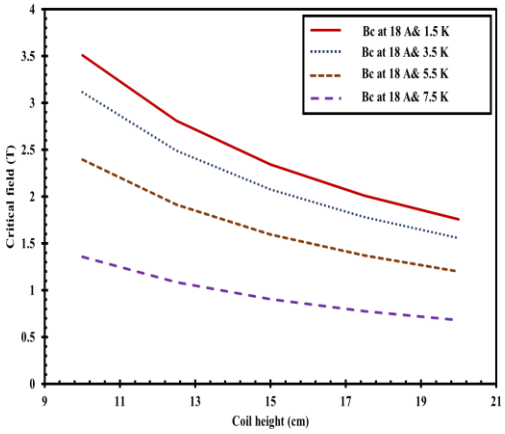

(c) Critical field at 18 A

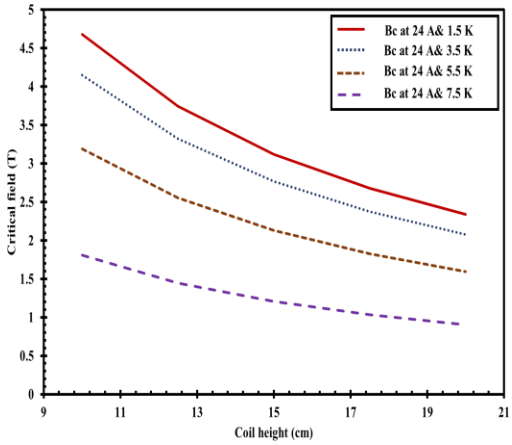

(d) Critical field at 24 A

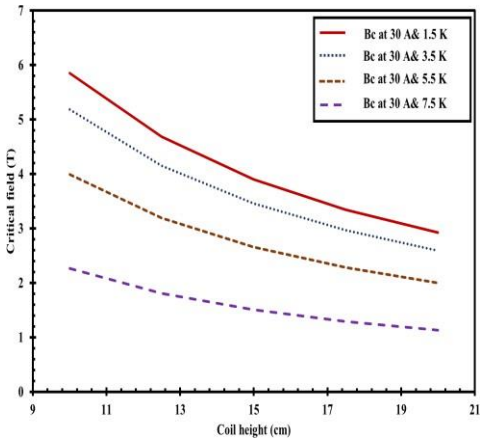

(e) Critical field at 30 A

Figure 6: Variation of critical field with coil height

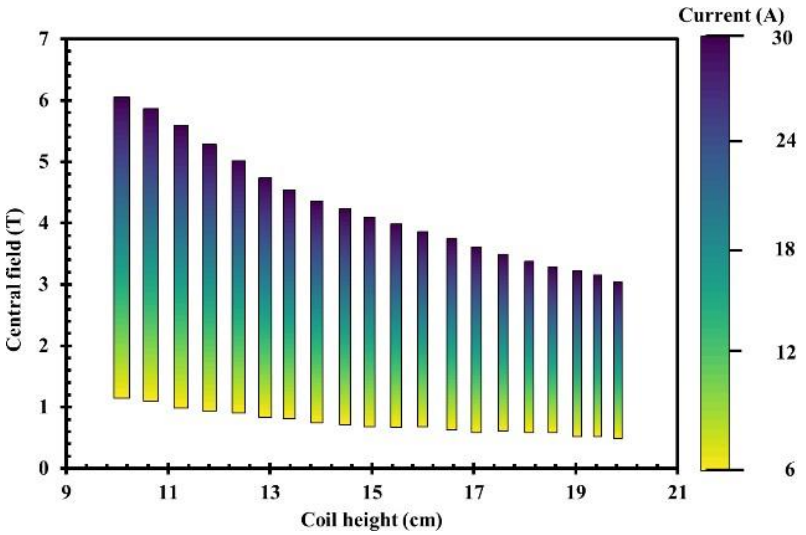

Figure 7: Variation of Central field with current

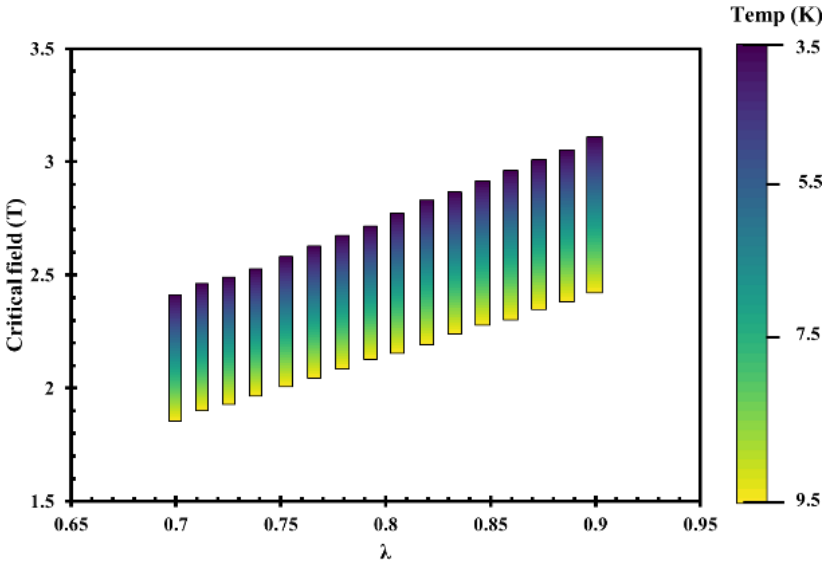

Figure 8: Variation of critical field with space factor

Based on optimal inlet condition (Table 2) and using the developed numerical model, the contours for analyzing the field distribution along the transverse and longitudinal directions of the superconducting magnet has been obtained for various superconducting alloy wires such as NbTi, Nb_3Al, NbZr and Nb_3Sn as shown in Fig. 9. Here, aforementioned alloy wires are chosen based on suitability at low cryogenic temperature of below 9.5 K. From this figure, it is found that NbTi alloy is best suitable as a superconducting wire compared to other alloys with a maximum possible central field of 10 T. This due to good stability at high magnetic fields. In addition, it is also found that maximum distribution of magnetic field is concentrated at central region and minimum field distribution is observed at the corners of the superconducting magnet along the transverse and longitudinal directions for all the alloy wires. It happens because the magnetic field lines inside the solenoid/former of superconducting magnet are homogeneous, densely packed, and converging which results in greater magnetic field at the centre portion than in any other region.

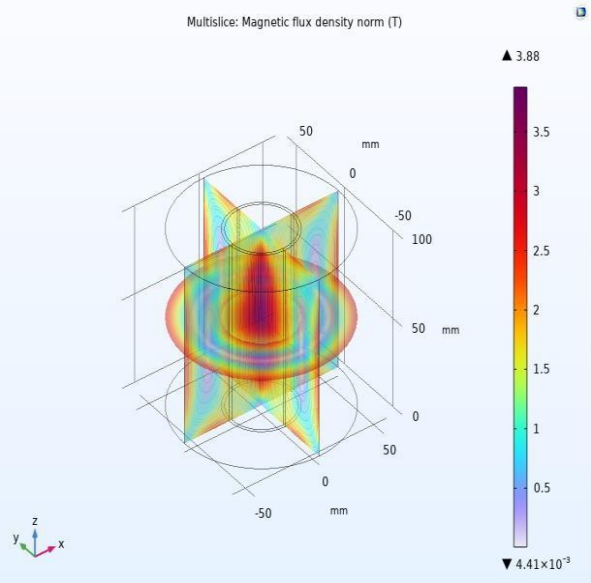

(a) 304 SS with NbTi SC wire 3.88 T

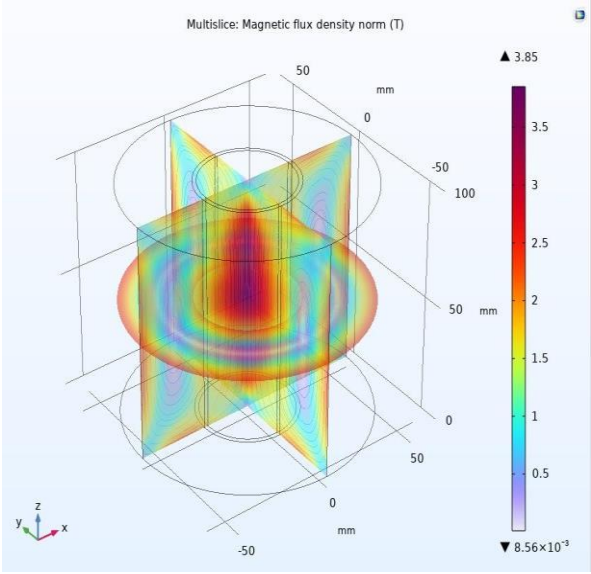

(b) 304 SS with Nb3Al Sc wire 3.85 T

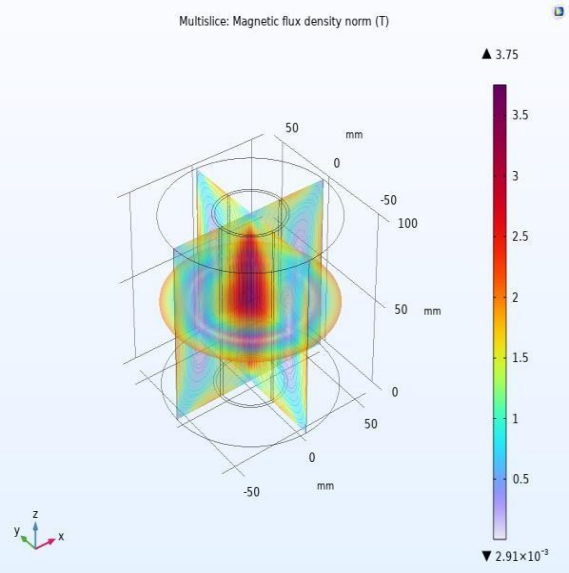

(c) 304 SS with NbZr Sc wire 3.75 T

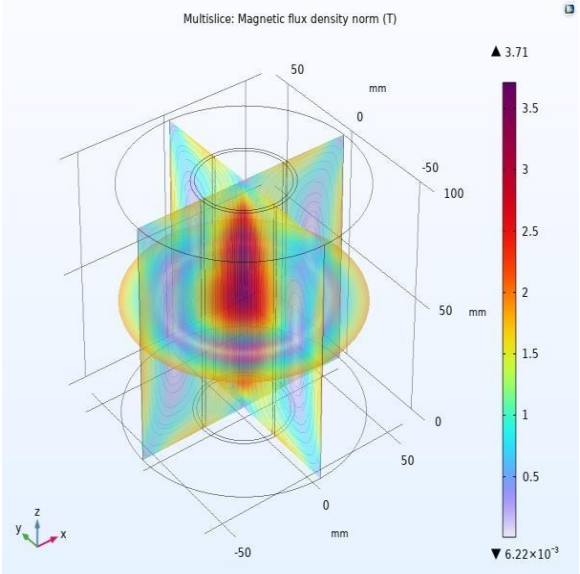

(d) 304 SS with Nb3Sn Sc wire 3.71 T

Figure 9: COMSOL Multislice plots for different SC alloy wires

6. CONCLUSIONS

Two models were developed (viz., analytical, and numerical) for predicting the performance and for parametric investigation on superconducting magnet. The developed models were validated with the experimental data provided in the literature and found good agreement with reasonable accuracy. In this study, NbTi alloy and SS304L are considered as superconducting alloy wire and solenoid/former material, respectively. Using the developed analytical model influence of inlet parameters such as coil height, current, space factor and cryogenic temperature on performance parameters such as central field, number of turns and critical field are investigated in detail. From the parametric study, it is found that low cryogenic temperature and coil height as well as high current and space factor yields better performance of superconducting magnet. Further, an optimal operating condition is predicted by observing 6 T as the maximum central field for the given inlet condition. Moreover, using the optimal inlet condition and

developed numerical model, the performance of the superconducting magnet for NbTi, Nb_3Al, NbZr and Nb_3Sn alloy wires are predicted and observed that NbTi alloy wire is preferred at low cryogenic temperature of below 9 K for providing high central field strength.

ACKNOWLEDGEMENT

This work is carried as a part of the on-going technology development project entitled “Design and Development of Magneto Resistive Heat Switch”. This project is supported by the SAC, Ahmedabad, ISRO, Government of India, Project Number No. YS/PD-IP/2021/364.

REFERENCES

1. Schmalian, J., 2010. “Failed theories of superconductivity”. Modern Physics Letters B, Vol. 24, issue 27, pp.2679-2691.
2. Mess, K. H., Schmüser, P. and Wolf S., 1996. “SUPERCONDUCTING ACCELERATOR MAGNETS” World Scientific.
3. A.C. Rose-Innes, E.H. Rhoderidz, 1969. “Introduction to Superconductivity” Pergamon Press, Library of Congress Catalog Card No. 79-78591.
4. Bardeen, J., Cooper, L.N. and Schrieffer, J.R., 1957 “Theory of superconductivity”. Phys. Rev. Vol. 108 issue 5, pp 1175—1204.
5. Leung, E.M.W., Hilal, M.A., Parmer, J.F., and Peck, S.D., 1987 “Light weight magnet for space application’s” Vol. MAG-2.
6. J. 0. Betterton, Jr., 1961. "Superconductivity of Nb_3Sn in a pulsed magnetic field," Phys. Rev. Lett., vol. 6, pp. 532-534.
7. R, G, Sharma, 2021. “Superconductivity: Basics and applications to magnets”. Vol. 214. Springer Nature
8. P.W. Anderson, J.M. Rowell, 1963. Phys. Rev. Lett. “Probable Observation of the Josephson Superconducting Tunneling Effect” Vol. 10, issue 6, pp 230.
9. T. G. Berlincourt, 1961. "Superconductivity at high magnetic fields and current densities in some Nb-Zr alloys," Phys. Rev. Lett., Vol. 6, pp. 671-674.
10. Marchevsky M., 2017 “Protection of superconducting magnet circuits” USPAS.
11. Ferracin, P., 2017 “Design of Superconducting magnets for particle accelerators and detectors” EUCAS.
12. Sullivian, D.B., & Vorreiter, J.W., 1979. “Space applications of superconductivity” CRYOGENICS Vol. 19, pp 627-631.
13. Jang, J. Y., Kim, M. S., Hwang, Y. J., Song, S., Choi, Y. and Choi, Y. S., 2021 “Development of a Cryogen-Free Compact 3 T Superconducting Magnet for an Electromagnetic Property Measurement System” Applied Science. 11(7), 3074.
14. Ledbetter, H. M., Weston, W. F., and Naimon, E. R., 1975 “Low temperature elastic properties of four austenitic stainless steels” Journal of Applied Physics Vol. 46, 3855-3860.
15. Roy, S., Konar, G., 2012. “Simulation of Flux Density in a Hybrid Coil Superconducting Magnetic Energy Storage Using COMSOL Multiphysics” COMSOL Conference in Bangalore.
16. Iwasa, Y., 2009. “Case Studies in Superconducting Magnets: Design and Operational Issues”, Chapter 3, pp 101-148 Springer.